Modelling Fluorescent Materials with a Spectral Overlap between Excitation and Emission Spectrum

Sven Leyre[1,2,3], Martijn Withouck[1,2], Guy Durinck[1,2,3], Geert Deconinck[2] and Peter Hanselaer[1,2,3]
[1]*Light & Lighting Laboratory, KU Leuven, Gebroeders Desmetstraat 1, Leuven, Belgium*
[2]*ESAT/ELECTA, KU Leuven, Kasteelpark Arenberg 10, bus 2445, Leuven, Belgium*
[3]*SIM (Flemish Strategic Initiative on Materials), SOPPOM program, Technologiepark 935, Zwijnaarde, Belgium*

Keywords: Modelling, Fluorescence, Adding-doubling.

Abstract: The adding-doubling method can be used to determine the reflection and transmission characteristics of fluorescent materials. In this work, the method was adapted to allow the implementation of fluorescent particles with a significant overlap between excitation and emission spectrum. The proposed method was validated by comparing its results to the simulation results of traditional Monte Carlo ray tracing. The average difference over the visible wavelength range between the two methods was found to be smaller than 0.5%. The proposed adding-doubling method was adapted for the simulation of a blue light-emitting diode with a remote phosphor converter containing YAG:Ce phosphor. It was shown that it is important to take the spectral overlap between excitation and emission spectrum into account to determine the colour characteristics with sufficient accuracy.

1 INTRODUCTION

The adding-doubling (AD) method is a commonly used evaluation method to quickly determine the reflection and transmission characteristics of a stack of homogeneous plane parallel layers (Wiscombe, 1969; Hansens, 1969; Prahl *et al*, 1993). The layers may contain both surface and bulk scattering. Recently, the method was extended for fluorescent layers (Leyre *et al*, 2012). The method however does not allow a spectral overlap between excitation and emission spectrum of the fluorescent material. This can be a problem for e.g. the prediction of colour characteristics in lighting.

In white light-emitting diodes (LED) light sources, blue LEDs are usually combined with a yellow phosphor to obtain white light (Liu *et al*, 2010; Lee & Lee, 2006). The most commonly used phosphor for LED applications is the Yttrium Aluminium Garnet doped with Cerium (YAG:Ce). This phosphor has a significant spectral overlap between excitation and emission spectrum. At high concentrations of the phosphor, this will cause a red shift of the emitted spectrum, due to re-absorption effects in the phosphor (Dhami *et al*, 1995). It is thus important to take the spectral overlap between excitation and emission spectrum into account when predicting the colour properties of an LED light source.

In this paper, an improved version of the adding-doubling method for fluorescent layers is presented, which allows the implementation of fluorescent layers with a spectral overlap between excitation and emission spectrum. First, the theoretical background for the improved adding-doubling method is presented, next the method is validated by comparing the results with traditional Monte Carlo ray tracing simulations. Finally, the significance of the spectral overlap is shown by comparing the predicted colour properties with and without the overlap taken into account of a blue LED incident on a remote phosphor converter containing YAG:Ce.

2 THEORETICAL BACKGROUND

The AD method was first developed by Stokes (Stokes, 1862) and allows the calculation of reflection and transmission of a stack of layers. The method has been adapted to allow the calculation of reflection and transmission of a homogeneous plane

Leyre S., Withouck M., Durinck G., Deconinck G. and Hanselaer P..
Modelling Fluorescent Materials with a Spectral Overlap between Excitation and Emission Spectrum.
DOI: 10.5220/0004729700330038
In *Proceedings of 2nd International Conference on Photonics, Optics and Laser Technology* (PHOTOPTICS-2014), pages 33-38
ISBN: 978-989-758-008-6

parallel slab containing bulk scattering (Wiscombe, 1969) and has found its way to the astronomy (Hansen, 1969) and bio-medical field (Saeys *et al*, 1993). Recently, the method was adapted to allow calculation of reflection and transmission of a fluorescent layer (Leyre *et al*, 2012). The main advantage of the AD method over e.g. Monte Carlo ray tracing simulations is that the AD method is much quicker. The Monte Carlo approach has the advantage that it is not limited to plane parallel geometries.

The AD method departs from the radiative transfer equation (RTE), representing the light propagation through a fluorescent layer, given by Equation 1.

$$\mathbf{s}.\nabla L(\mathbf{r},\mathbf{s},\lambda_M) = -(\mu_a+\mu_s).L(\mathbf{r},\mathbf{s},\lambda_M) + \mu_s.\int_{4.\pi} p(\mathbf{s},\mathbf{s}').L(\mathbf{r},\mathbf{s}',\lambda_M).d\Omega' + w_M(\lambda_M).\sum_{i=1}^{N}\left\{\mu_e(\lambda_{X_i}).QE(\lambda_{X_i}).\left[\int_{4.\pi} L(\mathbf{r},\mathbf{s}',\lambda_{X_i}).d\Omega'\right].\Delta\lambda_{X_i}\right\} \quad (1)$$

In words, this equation represents the change in spectral radiance $L(\mathbf{r},\mathbf{s},\lambda_M)$ at position $\mathbf{r}$ in direction $\mathbf{s}$. The first term on the right hand side represents the spectral radiance lost due to absorption and scattering, the second term is the contribution in the selected direction $\mathbf{s}$ from all other directions $\mathbf{s}'$ integrated over solid angle $d\Omega'$, and the third term is the contribution at wavelength λ_M from all excitation wavelengths, where the excitation wavelength region is divided into N wavelength intervals with central wavelength λ_{Xi}.

In Equation 1, μ_a and μ_s are the absorption and scattering coefficient and define the average distance travelled by a photon before being absorbed and scattered respectively. The phase function $p(\mathbf{s},\mathbf{s}')$ gives the probability a photon will be scattered in a certain direction. If the scattering occurs isotropically, $p(\mathbf{s},\mathbf{s}')$ is a constant. A commonly used phase function is the Henyey-Greenstein phase function, which has one free parameter: the anisotropy factor g, which is identical to the average of the cosine of the scatter angle (Henyey & Greenstein, 1941).

The factor $w_M(\lambda_M)$ is the weight of the selected wavelength within the emission spectrum, QE is the quantum efficiency of the fluorescent material, $\mu_e(\lambda_{Xi})$ is the excitation coefficient. If the selected wavelength λ_M is not included in the spectral emission band of the material, the third term on the right hand side of Equation 1 disappears ($w_M(\lambda_M)$ is zero) and the RTE for non-fluorescent materials is obtained (Leyre *et al*, 2012).

In the AD method, the incident radiance on a material is divided into cones or channels, which can be mathematically represented as a vector, where each element in the vector represents the radiance within a channel. The reflection and transmission characteristics are represented in matrices, allowing the radiance to be distributed over the different channels.

Equation 2 gives the mathematical representation of the transmission of the spectral radiance through a slab (Wiscombe, 1969).

$$\begin{bmatrix} L_1(\theta_1) \\ \vdots \\ L_1(\theta_n) \end{bmatrix} = \begin{bmatrix} T_{01}(\theta_1,\theta_1) & \cdots & T_{01}(\theta_1,\theta_n) \\ \vdots & & \vdots \\ T_{01}(\theta_n,\theta_1) & \cdots & T_{01}(\theta_n,\theta_n) \end{bmatrix} . \begin{bmatrix} L_0(\theta_1) \\ \vdots \\ L_0(\theta_n) \end{bmatrix} \quad (2)$$

With L_0 being the incident spectral radiance and L_1 the transmitted spectral radiance. The radiance is divided into n channels (represented by the corresponding polar angle θ). The matrix elements $T_{xy}(\theta_a,\theta_b)$ represent the light propagation from spectral radiance at position x, channel a to spectral radiance at position y, channel b. Equation 2 can also be written as $\mathbf{L}_1=\mathbf{T}_{01}.\mathbf{L}_0$, with $\mathbf{L}_0$ and $\mathbf{L}_1$ being the spectral radiance vectors and $\mathbf{T}_{01}$ the transmission matrix.

When dealing with fluorescent layers, the radiance is not only redistributed angularly, but also spectrally. The spectral radiance at wavelengths included in the spectral emission band, has contributions from all spectral radiances included in the spectral excitation band. Leyre *et al* (2012) used 'conversion matrices' to handle the spectral redistribution of the spectral radiance (mathematically represented in Equation 3).

$$\mathbf{L}_1(\lambda_M) = \mathbf{T}_{01}.\mathbf{L}_0(\lambda_M) + \sum_{i=1}^{N}\mathbf{T}^c_{01}(\lambda_{X_i},\lambda_M).\mathbf{L}_0(\lambda_{X_i}) \quad (3)$$

In Equation 3, $\mathbf{L}_0(\lambda_M)$ and $\mathbf{L}_1(\lambda_M)$ are the incident and transmitted spectral radiance at emission wavelength λ_M respectively, $\mathbf{L}_0(\lambda_{Xi})$ is the incident spectral radiance at excitation wavelength λ_{Xi} and $\mathbf{T}^c_{01}(\lambda_{Xi}, \lambda_M)$ is the conversion matrix, representing the fluorescent contribution at wavelength λ_M from wavelength λ_{Xi} in the forward direction. Each wavelength within the excitation wavelength region will contribute to the emission at wavelength λ_M, this is represented by the summation in Equation 3, where the excitation wavelength region is divided into N wavelength intervals with central wavelength λ_{Xi}.

To calculate the reflection and transmission through a layer which contains bulk scattering or fluorescence, the AD method starts from a thin 'single scatter' layer. The thickness of the layer is chosen in such a way that a photon will only interact a single time with the material. The reflection and transmission characteristics of this 'single scatter'

layer are determined with the RTE, given in Equation 1. Next, the layer is doubled in size, by adding two identical layers together and calculating the reflection and transmission. This step is repeated until the desired thickness is reached. A more elaborate explanation of the AD method can be found in (Leyre *et al*, 2012).

The AD method starts from Equations 4 and 5, representing the relationship between the upward and downward spectral radiance at each side of a single layer.

$$\mathbf{L}_1^+(\lambda_M) = \mathbf{R}_{10}.\mathbf{L}_1^-(\lambda_M) + \mathbf{T}_{01}.\mathbf{L}_0^+(\lambda_M) + \sum_{i=1}^{N} \mathbf{R}_{10}^e(\lambda_{X_i}, \lambda_M).\mathbf{L}_1^-(\lambda_{X_i}) + \mathbf{T}_{01}^e(\lambda_{X_i}, \lambda_M).\mathbf{L}_0^+(\lambda_{X_i}) \quad (4)$$

$$\mathbf{L}_0^-(\lambda_M) = \mathbf{R}_{01}.\mathbf{L}_0^+(\lambda_M) + \mathbf{T}_{10}.\mathbf{L}_1^-(\lambda_M) + \sum_{i=1}^{N} \mathbf{R}_{01}^e(\lambda_{X_i}, \lambda_M).\mathbf{L}_0^+(\lambda_{X_i}) + \mathbf{T}_{10}^e(\lambda_{X_i}, \lambda_M).\mathbf{L}_1^-(\lambda_{X_i}) \quad (5)$$

Herein, the superscripts '+' and '-' represent the spectral radiance going down- and upwards respectively. The subscript '0' and '1' for the radiances represent the spectral radiance on top and at the bottom of the layer respectively. For the reflection and transmission matrices, the first number of the subscripts denotes the incoming direction of the redistributed radiance (e.g. $\mathbf{R}_{01}$ represents the reflection matrices for light incident on the top of the layer). If the wavelength does not fall within the emission wavelength region, the third and fourth term on the right hand side of Equations 4 and 5 will disappear, since the conversion matrices are null matrices.

The AD method combines Equations 4 and 5 to obtain the reflection and transmission characteristics of the doubled layer. It inherently assumes that all radiances at wavelengths λ_{Xi} are not included in the emission wavelength region, i.e. the conversion matrices in Equations 4 and 5 are null matrices for all λ_{Xi} (Leyre *et al*, 2012). The result of this approach is that fluorescent materials with an overlap between excitation and emission wavelength region, where re-absorption (and re-emission) of converted photons can occur, cannot be adequately treated.

To solve this problem, we propose to write the spectral radiance in vector form for the full spectrum instead of one vector for each wavelength. As a result, the reflection and transmission matrices will allow the conversion of wavelength (both up- and down-conversion) without the need for special conversion matrices. Equation 6 now replaces the equations for each individual wavelength given by Equation 3.

Equation 6 allows both angular and spectral redistribution of light with a single matrix. Using the new vector-matrix notation, the third and fourth term on the right hand side of Equations 4 and 5 become obsolete (since the conversion matrices are no longer required). It is now much easier to obtain the reflection and transmission characteristics of a double layer, by combining Equations 4 and 5. The condition that the excitation wavelengths cannot be emission wavelengths as well, is no longer relevant. This allows to obtain the reflection and transmission characteristics of two combined layers which have a spectral overlap between excitation and emission wavelength region. Equations 4 and 5 (without the third and fourth term on the right hand side) can be written for two separate second layers. Combining the equations for the two layers leads to the reflection and transmission matrices for the combined layer, given by Equations 7 and 8.

$$\mathbf{R}_{20} = \mathbf{R}_{21} + \mathbf{T}_{12}(\mathbf{E} - \mathbf{R}_{10}\mathbf{R}_{12})^{-1}\mathbf{R}_{10}\mathbf{T}_{21} \quad (7)$$

$$\mathbf{T}_{02} = \mathbf{T}_{12}(\mathbf{E} - \mathbf{R}_{10}\mathbf{R}_{12})^{-1}\mathbf{T}_{01} \quad (8)$$

Herein, $\mathbf{E}$ is the unity matrix. To obtain the transmittance and reflectance of a layer, the incident radiance vector ($\mathbf{L}_0$) in Eq. 6 must be given the value '1' for the correct angles and wavelengths. The transmitted radiance vector ($\mathbf{L}_1$) can be calculated using Eq. 6. The transmittance at each wavelength can be calculated by integration over the different angles of the radiance represented in the transmitted radiance vector. In a similar way the reflectance can be obtained.

3 COMPARISON BETWEEN THE AD METHOD AND MONTE CARLO SIMULATIONS

To validate the method described in section 2, the results of the AD method are compared with traditional Monte Carlo ray tracing simulations. For

$$\begin{bmatrix} L_1(\theta_1,\lambda_1) \\ \vdots \\ L_1(\theta_n,\lambda_1) \\ \vdots \\ L_1(\theta_1,\lambda_N) \\ \vdots \\ L_1(\theta_n,\lambda_N) \end{bmatrix} = \begin{bmatrix} T_{01}(\theta_1,\lambda_1,\theta_1,\lambda_1) & \cdots & T_{01}(\theta_1,\lambda_1,\theta_n,\lambda_1) & \cdots & T_{01}(\theta_1,\lambda_1,\theta_1,\lambda_N) & \cdots & T_{01}(\theta_1,\lambda_1,\theta_n,\lambda_N) \\ \vdots & & \vdots & & \vdots & & \vdots \\ T_{01}(\theta_n,\lambda_1,\theta_1,\lambda_1) & \cdots & T_{01}(\theta_n,\lambda_1,\theta_n,\lambda_1) & \cdots & T_{01}(\theta_n,\lambda,\theta_1,\lambda_N) & \cdots & T_{01}(\theta_n,\lambda_1,\theta_n,\lambda_N) \\ \vdots & & \vdots & & \vdots & & \vdots \\ T_{01}(\theta_1,\lambda_N,\theta_1,\lambda_1) & \cdots & T_{01}(\theta_1,\lambda_N,\theta_n,\lambda_1) & \cdots & T_{01}(\theta_1,\lambda_N,\theta_1,\lambda_N) & \cdots & T_{01}(\theta_1,\lambda_N,\theta_n,\lambda_N) \\ \vdots & & \vdots & & \vdots & & \vdots \\ T_{01}(\theta_n,\lambda_N,\theta_1,\lambda_1) & \cdots & T_{01}(\theta_n,\lambda_N,\theta_n,\lambda_1) & \cdots & T_{01}(\theta_n,\lambda_N,\theta_1,\lambda_N) & \cdots & T_{01}(\theta_n,\lambda_N,\theta_n,\lambda_N) \end{bmatrix} \cdot \begin{bmatrix} L_0(\theta_1,\lambda_1) \\ \vdots \\ L_0(\theta_n,\lambda_1) \\ \vdots \\ L_0(\theta_1,\lambda_N) \\ \vdots \\ L_0(\theta_n,\lambda_N) \end{bmatrix} \quad (6)$$

the calculations and simulations, a plastic remote phosphor converter is modelled. The converter has optical flat surfaces (only Fresnel reflections at the air-converter interfaces), has refractive index of 1.5, thickness of 1 mm, and contains YAG:Ce phosphor particles. The phosphor particles cause scattering and fluorescence, the optical properties are taken from (Liu *et al*, 2010).

At a concentration of 0.2 g/cm³, the average scattering coefficient μ_s over the visible wavelength range is 25.71 mm^{-1}, and the average anisotropy factor g is 0.863. For the modelling the Henyey-Greenstein phase function is selected, since this allows for easy implementation in the AD method (Joseph & Wiscombe, 1976). The absorption and emission spectrum of the phosphor are shown in Figure 1. An obvious spectral overlap between excitation and emission spectrum can be noticed, which makes this phosphor an excellent candidate to validate the proposed AD method.

The peak absorption at 470 nm at concentration 0.2 g/cm³ is 1.79 mm-1. The QE of the phosphor is 0.87. The phosphor converter is illuminated with a blue LED, with peak wavelength 460 nm. The spectral radiant flux of the LED is represented in Figure 1.

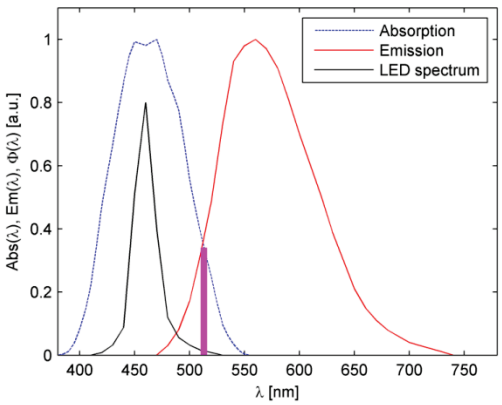

Figure 1: Absorption (blue dashed line) and emission spectrum (full red line) of the YAG:Ce phosphor, together with the spectral radiant flux of the blue LED (full black line). The thick vertical line represents the cut-off for excitation and emission spectrum if the spectral overlap is not taken into account.

The Monte Carlo simulations are performed with the software package TracePro. In this software, Fresnel reflections are handled by attributing a probability to each ray to be reflected or transmitted at an interface according to the Fresnel reflection and transmission coefficients. The volume scattering is handled by use of the scattering coefficient and the anisotropy factor, which can be introduced in the program for each wavelength. The fluorescence is handled by tracing the source from short to long wavelengths. The rays absorbed in the fluorescent material are stored to the hard disk. When an emission wavelength is reached, the absorbed rays are converted to the emission wavelength and given the appropriate radiant flux. This approach differs from the standard ray tracing procedure for fluorescence in the TracePro software and allows for the simulation of fluorescent materials with a spectral overlap.

The simulations and calculations are performed between 380 and 780 nm and in steps of 5 nm, the concentration of phosphor in the converter is 0.2 g/cm³. The Monte Carlo simulation is performed with 100 000 rays per wavelength. In Figure 2, the result of the Monte Carlo simulation and the AD calculations is shown, together with the relative deviation between the two methods.

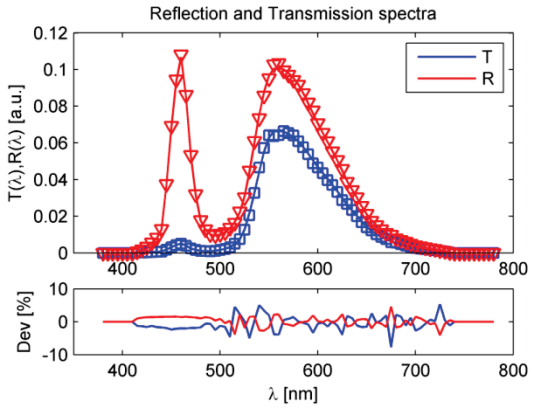

Figure 2: Comparison between the AD method (lines) and Monte Carlo simulations (marks) for the transmitted spectrum T (triangles) and the reflected spectrum R (squares), together with the relative deviation (dev) between the two methods.

From Figure 2, it can be seen that there is only a very small deviation between the AD calculations and the Monte Carlo simulations. The average relative deviation is smaller than 0.5%. Moreover, given the random variation of the deviation over the wavelengths, it can be attributed to noise in the Monte Carlo simulations. It can be concluded that the AD method can indeed be used to calculate reflection and transmission of a fluorescent component with a spectral overlap between excitation and emission spectrum. The AD method takes approximately 90 seconds for the full calculations, the Monte Carlo simulations takes approximately 15 hours. The AD method thus decreases the computation time with a factor 600 (for Monte Carlo simulations with 100.000 rays per wavelength).

4 SIMULATION OF A REMOTE PHOSPHOR APPLICATION

In the previous section, it was shown that the AD method can be used for the quick calculation of the transmitted spectrum through a remote phosphor converter. Now, the influence of the spectral overlap of the excitation and emission spectrum on the colour characteristics of the remote phosphor device will be investigated by comparing the CIE 1931 *x,y* chromaticity coordinates of the transmitted spectrum with and without the spectral overlap taken into account. When the spectral overlap is not taken into account, the excitation and emission spectrum are cut off at 510 nm (shown in Figure 1). The concentration of phosphor in the remote phosphor converter is varied, to show the influence of the concentration on the difference with and without spectral overlap taken into account. In Figure 3, the chromaticity coordinates are represented in the CIE 1931 *x,y* chromaticity diagram, for a concentration of 0.01, 0.02, 0.035, 0.05, 0.065, 0.08, 0.1, 0.15, 0.4 g/cm³ YAG:Ce in the remote phosphor converter.

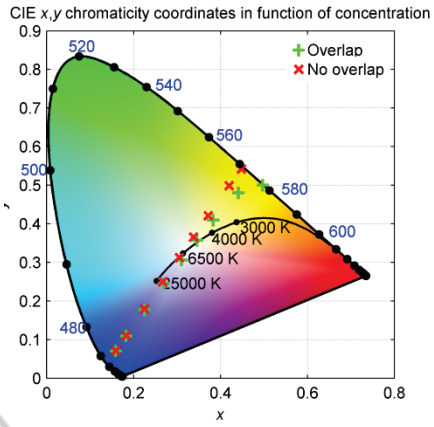

Figure 3: CIE 1931 *x,y* chromaticity coordinates of the simulated transmitted spectrum for different concentrations of YAG:Ce in the remote phosphor converter, with (+) and without (x) the spectral overlap between excitation and emission spectrum taken into account.

From Figure 3, an obvious deviation in chromaticity coordinates is noticeable, especially at high concentrations of the phosphor. When the spectral overlap is not taken into account, the chromaticity coordinates for various concentrations of phosphor are on a straight line. In this case, the 'blue' (from the LED) and 'yellow' (from the phosphor) part of the spectrum have a fixed spectral distribution, only the ratio of the 'blue' and 'yellow' part changes. When the spectral overlap is taken into account, the 'yellow' part of the spectrum is not constant, since re-absorption effects will red-shift the 'yellow' part. At low concentrations, the red-shift effect is less pronounced, since the probability of re-absorption events to occur is much lower at lower concentrations.

At a concentration of 0.08 g/cm³, the chromaticity coordinates for the simulated spectrum with the spectral overlap taken into account are closest to the Planckian locus. The Correlated Colour Temperature (CCT) is 5007 K. For the same concentration, the simulated spectrum without the spectral overlap taken into account results in a CCT of 5313 K. The distance between the two simulated colours is larger than a nine-step Mac Adam ellipse (MacAdam, 1942). According to the recent regulations of the European Commission regarding LED lamps, the colour consistency of light sources should be within a six-step Mac Adam ellipse (European Commission, 2012). The correct simulation of the spectral overlap between excitation and emission spectrum of the phosphors used in LED lamps is thus important to determine the colour

characteristics of the light source with sufficient accuracy.

The difference in luminous flux of the simulated source with and without spectral overlap taken into account is smaller than 3%, the effect on the colour characteristics is thus the dominant problem when ignoring the spectral overlap.

5 CONCLUSIONS

In the paper, the adding-doubling (AD) method was adapted to allow the calculation of reflection and transmission characteristics of plane parallel fluorescent layers with a spectral overlap between excitation and emission spectrum. The proposed method was validated with traditional Monte Carlo ray tracing simulations, the deviation between the two methods was smaller than 0.5%. The computation time with the AD method was approximately 90 seconds, while the Monte Carlo simulations took 15 hours.

The AD method was used to calculate the transmitted spectrum through a remote phosphor converter containing YAG:Ce illuminated with a blue LED. It was shown that it is important to take the spectral overlap between excitation and emission spectrum into account to predict the colour characteristics of the remote phosphor application.

In the future, experiments on a plane parallel remote phosphor converter will be performed to verify the conclusions in this work. The presented method will also be adapted to perform colour calculations under different illumination geometries (e.g. an LED with a lambertian intensity distribution).

ACKNOWLEDGEMENTS

The authors would like to thank the SIM (Flemish Strategic Initiative for Materials) and IWT (Flemish agency for Innovation by Science and Technology) for their financial support through the SoPPoM project within the SIBO program.

REFERENCES

Dhami, S., de Mello, A. J., Rumbles, G., Bishop, S. M., Phillips, D., Beeby, A. (1995). Phthalocyanine fluorescence at high concentration: dimers or reabsorption effect? *Photochem. Photobiol.* 61 (4), 341-346.

European Commission (2012). *Commission Regulation (EU) No 1194/2012 of 12 December 2012 implementing Directive 2009/125/EC of the European Parliament and of the Council with regard to ecodesign requirements for directional lamps, light emitting diode lamps and related equipment.* Brussels, Official Journal of the European Union.

Hansen, J. E. (1969). Radiative transfer by doubling very thin layers. *Astrophys. J.* 155, 563-573.

Henyey, L. G., Greenstein, J. L. (1941). Diffuse radiation in the galaxy. *Astrophys. J.* 93, 70-83.

Joseph, J. H., Wiscombe, W. J. (1976). The Delta-Eddington Approximation for Radiative Flux Transfer. *J. Atmos. Sci.* 33, 2452-2459.

Lee K. H., Lee, S. W. R. (2006). Process development for yellow phosphor coating on blue light-emitting diodes (LEDs) for white light illumination. *8th Electronics Packaging Technology Conference,* Singapore, 6-8 December.

Leyre, S., Durinck, G., Van Giel, B., Saeys, W., Hofkens, J., Deconinck, G., Hanselaer, P. (2012). Extended adding-doubling method for fluorescent applications. *Opt. Express* 20 (16), 17856-17872.

Liu, Z., Liu, S., Wang, K., Luo, X. (2010). Measurement and numerical studies of optical properties of YAG:Ce phosphor for white light-emitting diode packaging. *Appl. Opt.* 49 (2), 247-257.

MacAdam, D. L. (1942). Visual Sensitivities to Color Differences in Daylight. *J. Opt. Soc. Am. A* 32 (5), 247-274.

Prahl, S. A., van Gemert, M. J. C., Welch, A. J. (1993). Determining the optical properties of turbid media by using the adding-doubling method. *Appl. Opt.* 32 (4), 559–568.

Saeys, W., Velazco-Roa, M. A., Thennadil, S. N., Ramon, H., Nicolaï, B. M. (2008). Optical properties of apple skin and flesh in the wavelength range from 350 to 2200 nm. *Appl. Opt.* 47 (7), 908-919.

Stokes, G. G. (1862). On the intensity of the light reflected from or transmitted through a pile of plates. *Proc. Roy. Soc. London* 11, 545–556.

Wiscombe, W. J. (1976). On initialization, error and flux conservation in the doubling method. *J. Quant. Spectrosc. Radiat. Transfer* 16, 637–658.